Systems Chemistry

Communication and Cross-Regulation between Chemically Fueled Sender and Receiver Reaction Networks**

Mo Sun,* Jie Deng, and Andreas Walther*

Abstract: Nature connects multiple fuel-driven chemical/enzymatic reaction networks (CRNs/ERNs) via cross-regulation to hierarchically control biofunctions for a tailored adaption in complex sensory landscapes. Herein, we introduce a facile example of communication and cross-regulation among two fuel-driven DNA-based ERNs regulated by a concatenated RNA transcription regulator. ERN1 ("sender") is designed for the fuel-driven promoter formation for T7 RNA polymerase, which activates RNA transcription. The produced RNA can deactivate or activate DNA in ERN2 ("receiver") by toehold-mediated strand displacement, leading to a communication between two ERNs. The RNA from ERN1 can repress or promote the fuel-driven state of ERN2; ERN2 in turn feedbacks to regulate the lifetime of ERN1. Furthermore, the incorporation of RNase H allows for RNA degradation and enables the autonomous recovery of ERN2. We believe that concatenation of multiple CRNs/ERNs provides a basis for the design of more elaborate autonomous regulatory mechanisms in systems chemistry and synthetic biology.

Introduction

Living systems organize structures and functions via hierarchically concatenated non-equilibrium chemical and enzymatic reaction networks (CRNs/ERNs).[1–9] Microtubules, designed for adaptive spatial search, are the most striking example for a fuel-driven CRN-based structure, continuously consuming guanosine triphosphate (GTP) as the energy to maintain a dynamic steady state (DySS) between polymerization and depolymerization. Then motor proteins, including kinesin and dynein, whose energy source is from adenosine triphosphate (ATP) hydrolysis, can bind and move along the microtubule tracks for directed cellular transportation. Again, these molecular motors are powered by a cyclic CRN consuming ATP. This connection of different entities powered by individual fuel-driven CRNs and running on different fuels gives rise to sophisticated biological functions, such as adaptation and transportation.

By taking inspiration from nature, there has been significant progress in the design of relatively simple, chemically fueled self-assemblies using CRNs and ERNs based on a diversity of fuels, building blocks and approaches.[10–23] However, connecting different fuel-driven modules and achieving cross-regulation is challenging. To this end, cross-regulation in more complex fuel-driven systems has for instance been previously shown by the PEN (polymerase/exonuclease/nickase) toolbox, in which multiple enzymatic reactions were concatenated and operated in tandem, leading to oscillations in a closed environment.[24–27] Moreover, synthetic RNA transcriptional oscillators have been achieved by regulating the transcription activity of two concatenated RNA transcription systems using the same chemistry.[28,29] Those systems have shown excellent applications in dynamic control of various self-assembly processes, such as colloid and DNA nanotube assemblies. Despite this progress, the modular cross-regulation of multiple concatenated ERNs is still rare, especially for systems using distinct chemistries.

We have recently developed a novel ATP-driven ERN system of concurrent ATP-fueled DNA ligation and digestion of sticky end functionalized DNA building blocks using T4 DNA ligase with various restriction endonucleases

[*] Dr. M. Sun
Department of Chemistry, Fudan University
Shanghai 200438 (China)
E-mail: mosun@fudan.edu.cn

Dr. J. Deng, Prof. Dr. A. Walther
Life Like Materials and Systems, Department of Chemistry,
University of Mainz
Duesbergweg 10–14, 55128 Mainz (Germany)
E-mail: andreas.walther@uni-mainz.de

Dr. M. Sun, Prof. Dr. A. Walther
Cluster of Excellence livMatS @ FIT – Freiburg Center for
Interactive Materials and Bioinspired Technologies, University of
Freiburg
Georges-Köhler-Allee 105, 79110 Freiburg (Germany)

Dr. J. Deng
Dana-Farber Cancer Institute, Wyss Institute for Biologically
Inspired Engineering, Harvard Medical School
Boston, MA 02115 (USA)

(REases).[30] The system shows high versatility including photo-activation of fuels and building blocks,[31] translation into hierarchical assemblies,[32,33] or pathway complexity.[34–38] Additionally, it was possible to connect ATP-driven structures with strand displacement reactions to provide first examples of isothermally self-resetting strand displacement cascades.[29] This demonstrates that a connection of reaction networks, i.e. ATP-driven DNA ERNs with strand displacement, can lead to new behaviors. However, one of the significant remaining challenges is to identify pathways for connecting multiple ATP-driven ERNs with fuel-dependent regulatory mechanisms, so as to achieve communication and feedback. This would allow for increasing behavioral complexity and promote capacity for adaptation in future systems.

Herein, we set out to address the challenge of achieving communication between two dynamic chemical systems by coupling chemical fuel-driven non-equilibrium DNA ERNs with an RNA transcription system to achieve cross-regulation and feedback (Scheme 1). The RNA transcription system is controlled by one ERN ("the sender") and only occurs in the fuel-driven non-equilibrium state. The produced RNA works as an ON or OFF switch for the second ERN ("the receiver"). This allows cross-regulation from a primary DNA-based ERN to a secondary DNA-based ERN by information exchange using co-transcribed RNA messenger. We describe various control modules (e.g. promotion, repression, recovery) that build on RNA-mediated strand displacement reactions on the building blocks of the receiver ERN, and we also show that addition of RNase H can lead to recovery of the behavior by digestion of the RNA messenger. The use of RNA opens the perspective to use orthogonal enzymes and chemo-specific degradation as control tools. We believe that these additional control mechanisms can help to promote regulatory functions, signal processing and adaptation capacity to future chemically instructed materials systems with life-like behavior.

Results and Discussion

Based on our recent study of non-equilibrium ERNs of ATP-fueled concurrent DNA ligation and digestion,[30,32,35] we show here a conditional RNA transcription, that is
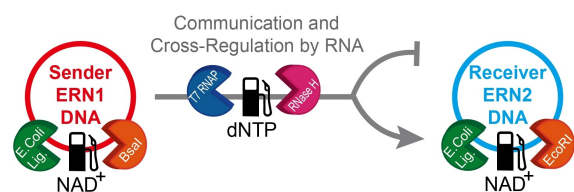

Scheme 1. General concept for RNA-based feedback regulation between two NAD+-fueled DNA-containing ligation/digestion enzymatic reaction networks (ERNs), termed Sender and Receiver. Communication and cross-regulation occur by RNA transcription from the fueled state of Sender. RNA production runs on dNTPs as fuels and degradation of RNA signals can occur if an RNase is present. The RNA signals can activate or suppress the Receiver network.

induced by the transient formation of the full DNA promoter sequence for T7 RNA polymerase (T7 RNAP) in the chemical fuel-driven state of a DNA-based ERN1. The transcribed RNA leads to a downstream regulation of a concatenated DNA-based ERN2. Our systems contain two ligation/digestion ERNs (1 and 2), termed according to their function as sender network (Sender) and receiver network (Receiver). Both Sender and Receiver follow a cyclic operation in an ERN driven by the fuel and enzymes (Scheme 2). The RNA transcription requires ribonucleotide triphosphates (NTP) as activated monomers.

First, we introduce the enzymes involved in the ERNs, as well as RNA transcription and degradation of this work. (1) Ligase: In contrast to our earlier work on ATP-driven cyclic ligation/digestion networks based on T4 DNA ligase, we herein introduce *E. coli* DNA ligase, that is able to ligate DNA fragments with 3′-OH and 5′-phosphate ends, but uses β-nicotinamide adenine dinucleotide (NAD+) instead of ATP (for T4 DNA ligase) as fuel. Using NAD+ prevents competition for the ATP fuel, because T7 RNAP also uses ATP during the transcription step. (2) REases: We specifically chose two different REases to minimize unwanted cross-talk between both ERNs (Sender and Receiver), and to highlight the importance of the RNA-regulators, as well as the fuel competition of both DNA ERNs. For Sender, we chose BsaI because BsaI allows for a free programmability of the restriction site that is located downstream of its recognition site.[32] For Receiver, we chose EcoRI with a fixed recognition and restriction site, because it is robust and efficient.[35] (3) T7 RNAP: The DNA-to-RNA transcription uses T7 RNAP, a DNA-dependent RNA polymerase, that is highly specific for specific promoters and runs on a NTP fuel mix (containing ATP, uridine triphosphate (UTP), GTP, cytidine triphosphate (CTP)). (4) RNase H: RNase H is used as RNase to specifically degrade RNA hybridized to DNA.

Second, we introduce the working principles of the Sender, and how its NAD+-driven operation can be coupled to RNA transcription. Similar to our previous report, the NAD+-driven DNA-based ERNs will form a transient DySS with a certain average degree of ligation as programmed by the ratio of the ligase and REases (as well as to a minor extent the concentration of the chemical fuel, NAD+).[30] The lifetime of the autonomous state is a function of the NAD+ concentration. In Sender, the monomeric DNA building block (M_S) contains a split T7 promoter sequence located at the α,ω-ends of M_S, as well as the full template coding the RNA messenger in the center. M_S is susceptible to dynamic covalent oligomerization (O_S) using the NAD+-driven ERN, which leads to the transient formation of the full promoter sequence. Hence, a complete promoter sequence is conditional on achieving the NAD+-fueled state (O_S state). This enables RNA transcription and the formation of RNA messengers used for downstream action on Receiver. In absence of NAD+, the RNA transcription does not occur, because the 4-nucleotide (nt) sticky overhang is too short for stable hybridization. Thus, the ligation state of Sender controls the ON-OFF switch of the
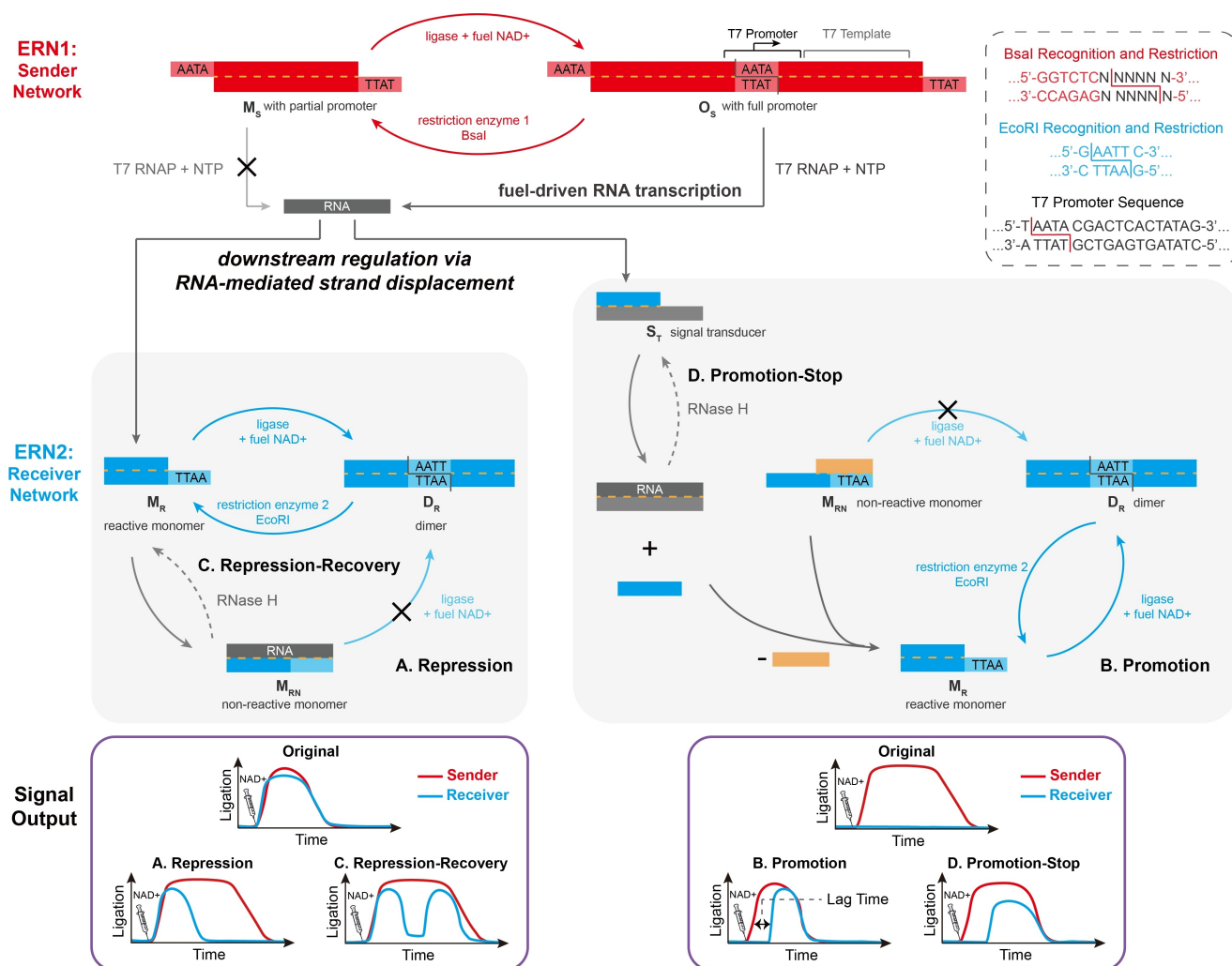
Scheme 2. Detailed working principle for RNA-based feedback regulation between two cyclic ligation/digestion networks.

transient RNA transcription via formation/deformation of the full T7 promoter.

Third, we introduce the working principle of the entire system and start with repression as the first example. Receiver is used to show the chemical information exchange between Sender and Receiver. Without RNA production from Sender (in absence of T7 RNAP), Receiver forms a similar DySS as Sender (Scheme 2—Original part in Signal Output). When RNA transcription is induced by addition of T7 RNAP and O_S formation in Sender, the transcribed RNA messenger is able to induce cross-talk with Receiver via RNA-mediated strand displacement, including four different results, that are repression, promotion, repression-recovery, and promotion-stop, based on the different sequence designs and enzymes. In the repression process (Scheme 2A), RNA is designed to transform the reactive monomer, M_R, into non-reactive monomer, M_{RN}, causing the shut-down of Receiver. Interestingly, since both Sender and Receiver run on the same fuel, their cross-activated behavior influences each other's transient lifecycles. For instance, in an activated repression process, the Receiver will have a shortened lifetime as forced by the produced RNA, while

concurrently, a longer lifetime of Sender should be achieved due to higher fuel (NAD^+) availability as the competition for the fuel is lost for by the suppressed Receiver (Scheme 2A and Signal Output part).

In contrast, in a promotion process (Scheme 2B), a non-reacting M_{RN} in Receiver exists at the beginning, and—only if RNA is produced—then M_{RN} transforms into M_R to start Receiver. Thus, in this promotion process, Receiver will experience a lag time in the cyclic operation compared to Sender and is also fully conditional on the presence of T7 RNAP. Additionally, Receiver starts to consume NAD^+ fuel as well, thus acting as a competitor for the Sender, giving a shorter lifetime of Sender.

Higher behavioral complexity is achievable by adding RNase H to degrade the RNA at the same. We will elucidate that this allows to switch the repression process into a repression-recovery process (Scheme 2C), because when the produced RNA is completely degraded, M_{RN} will be transformed back to M_R to restart Receiver. The addition of RNase H to the promotion process leads to a promotion-stop process (Scheme 2D), wherein the lag time of two ERNs will be tuned by the RNase amount.

We first focus on repression. More detailed design and analysis of the repressive signaling loop are illustrated as follows (Figure 1). In Sender, the Cy5-labeled DNA sequence of M_{S1} is designed to contain a BsaI recognition site (red part), a disconnected T7 promoter (black part), a T7 template (gray part), and a T7 RNAP run-off sequence (green). The ends of M_{S1} contain one 4-nt sticky end 5′-AATA-3′ on one side and the complementary sticky end 5′-TATT-3′ on the other side (detailed DNA sequences in Table S1). In relation to our previous work on ATP-driven ERNs,[37] M_{S1} can be transiently grown into an oligomeric DySS O_{S1}. During operation of the NAD$^+$-fueled cyclic ligation/digestion ERN, O_{S1} forms with the full T7 promoter sequence, and activates the RNA transcription. In Receiver, the fluorescein-labeled monomer (M_{R1}) is designed with a 4-

nt self-complementary sticky end 5′-AATT-3′ for ligation and EcoRI cutting, as well as with a segment F_{R1}, which can be removed by toehold-mediated strand displacement of the produced RNA. On its own and without considering the produced RNA, the presence of *E. coli* ligase/EcoRI and the fuel NAD$^+$ induces a transient DySS, in which M_{R1} will form a dimer D_{R1}, that is cut back to the monomer state after consumption of NAD$^+$. In absence of RNA transcription and strand displacement, these two ERNs of Sender and Receiver run independently, except sharing the fuel (NAD$^+$). The basic behavior of such ERNs has been reported previously.[35] In contrast, in presence of T7 RNAP, the produced RNA will displace the fluorescein-labeled strand F_{R1} through strand displacement, yielding a non-reactive DNA-RNA hybrid monomer M_{RN1}, which lacks the
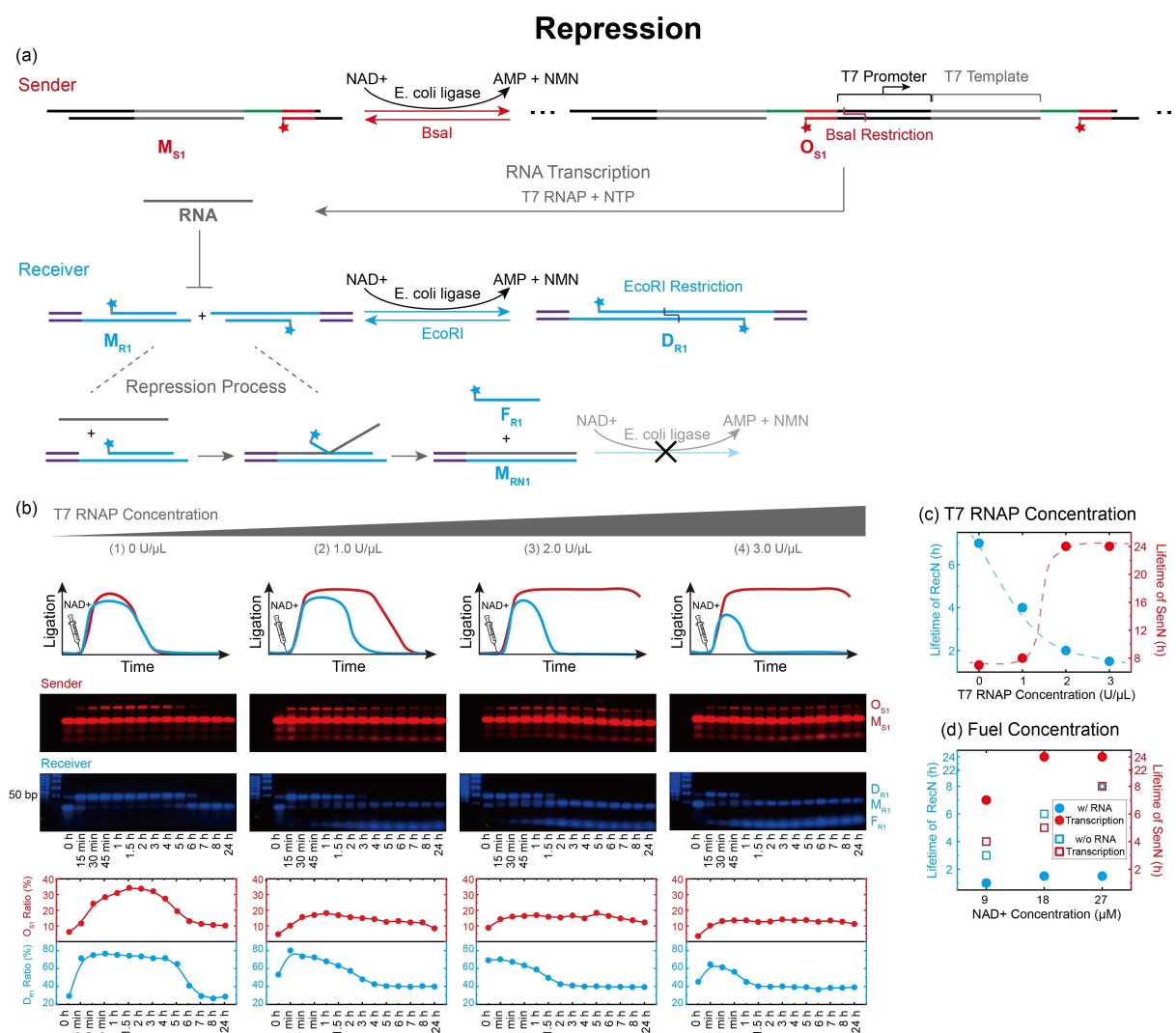

Figure 1. Repression. a) Schematic illustration of the repression process between two DNA-based ERNs (AMP for adenosine monophosphate; NMN for nicotinamide mononucleotide). b) Time-dependent transient polymerization curves and time-dependent evolution of O_{S1} ratio ($[O_{S1}]/([O_{S1}]+[M_{S1}])$) and D_{R1} ratio ($[D_{R1}]/([D_{R1}]+[M_{R1}]+[F_{R1}])$) as quantified by intensity analysis of the gel bands. c) Lifetime analysis of the repression process with [T7 RNAP]. Other conditions: 5.0 μM M_{S1}, 10.0 μM M_{R1}, 16.0 U μL^{-1} ligase, 0.67 U μL^{-1} EcoRI, 0.89 U μL^{-1} BsaI, 2.0 mM NTP, and 18.0 μM NAD$^+$. d) Lifetime analysis of the repression with [NAD$^+$]. Other conditions: 5.0 μM M_{S1}, 10.0 μM M_{R1}, 16.0 U μL^{-1} ligase, 0.67 U μL^{-1} EcoRI, 0.89 U μL^{-1} BsaI, 2.0 U μL^{-1} T7 RNAP, and 2.0 mM NTP. The minor red fluorescent bands at high migration distance correspond to some minor stochiometric imbalance.

sticky end for ligation. This process eventually stops Receiver.

Figure 1b displays the results of this repression process with multicolor agarose gel electrophoresis (AGE) of the time-dependent transient systems of Sender and Receiver at different [T7 RNAP]. The data can be simply quantified as a time-dependent evolution of O_{S1} ratio ($[O_{S1}]/([O_{S1}]+[M_{S1}])$) and D_{R1} ratio ($[D_{R1}]/([D_{R1}]+[M_{R1}]+[F_{R1}])$).

Overall both channels (Sender = red and Receiver = blue) show the individual transient systems, with the transient appearance of higher molecular weight species with a limited lifetime. In absence of RNA transcription (0 U μL^{-1} T7 RNAP), the lifetimes of the DySSs for red Sender and blue Receiver are very similar at about 6 h and 7 h (Figure 1b1). In the transient DySS (i.e. at 1–2 h), the monomeric band for M_{S1} is hardly visible, because the majority of M_{S1} is present as a dynamic dimer as first oligomeric species (O_{S1}). When adding 1.0 U μL^{-1} T7 RNAP, the Receiver lifetime decreases sharply to only 4 h, whereas the Sender shows an elongated plateau and an increased lifetime to ca. 8 h. At the same time, a new band corresponding to F_{R1} appears in AGE after 1.5 h, which originates from the RNA-induced strand displacement of F_{R1} from M_{R1}. Concurrently, the unreactive M_{RN1} is formed. By further increasing [T7 RNAP] to 2.0 U μL^{-1} and 3.0 U μL^{-1}, the lifetimes of Sender increase more significantly, to as long as 24 h, and, more critically, the lifetimes of Receiver shorten to 2 h and 1.5 h (Figures 1b3,4 and c). Concurrently, the F_{R1} band appears earlier and more pronounced, because the more T7 RNAP, the faster is RNA transcription and the faster is the formation of M_{RN1}. It should be noticed that the addition of T7 RNAP, besides changing the lifetimes, also increases the ligation ratio of Sender in the DySS because more NAD$^+$ fuel is available for the Sender due to repression of Receiver. This is shown in Figure S1, where the oligomerization of M_{S1} proceeds to clearly longer oligomers after adding 2.0 U μL^{-1} T7 RNAP. Note that for simplicity, we only show the monomer/dimer part of the AGE here.

To underscore the general tuneability of the system, the Supporting Information depicts related experiments for different [NAD$^+$] (Figures 1d, S2), as well as for different [NTP] (Figure S3). More NAD$^+$ increases the lifetimes of both Sender and Receiver and less NTPs weaken the repression due to fewer and slower RNA production.

To achieve the promotion process, we slightly modified the M_{S1} structure to M_{S2} to fit to the newly needed Sender/Receiver combination. The building block in Receiver is redesigned into an unreactive monomer, M_{RN2}, in which the reactive, self-complementary sticky ends for ligation are shielded by short complementary strands (orange, Figure 2a). Additionally, a signal transducer, S_T, is present, that can convert the generated RNA into an output activating M_{RN2} by strand displacement of the short, orange shielding strand. The translated signal carries a fluorescent dye fluorescein, so that its transfer into the activated monomer M_{R2} and subsequent dimerization in the cyclic ERN can be visualized in the blue channel. If there is no transcription, only Sender runs as a fuel-driven ERN. If the transcription

is switched on, M_{R2} generated by downstream strand displacement of M_{RN2} via the produced RNA enters the cyclic ligation/digestion ERN in Receiver. This delayed activation of Receiver concurrently is expected to reduce the lifetime of Sender compared to no transcription conditions due to competition for the NAD$^+$ fuel for the ligase. We first investigated the effect of [T7 RNAP] on this promotion process (Figures 2b,c). In absence of T7 RNAP, the lifetime of Sender is over 8 h (red channel), and a major single fluorescent band is visible in the blue channel corresponding to intact S_T (note that some minor unavoidable leakage happens). When gradually increasing [T7 RNAP] from 1.0 to 3.0 U μL^{-1}, Receiver becomes continuously activated. At 1.0 U μL^{-1} the band corresponding to the activated monomer M_{R2} clearly forms, but a dimerization is hardly visible (blue channel; Figure S4). Clear dimerization occurs for higher [T7 RNAP], which leads to sufficient RNA production for a complete signal conversion from S_T to M_{R2} and ensuing DySS dimerization in Receiver. The lag times decrease from 45 min (2.0 U μL^{-1} T7 RNAP) to 15 min (3.0 U μL^{-1} T7 RNAP), but clearly there are kinetic delays due to the need for signal translation. Concurrently, the lifetimes of Sender decrease from 5 to 3 h, and the lifetimes of Receiver synchronize, because the same stop time is set when the fuel NAD$^+$ in the solution is used up. Considering S_T and M_{RN2} to be the key components in this promotion process, we studied the influence of their ratio (Figures 2d,e). At the same concentration of M_{S2} and M_{RN2} (10.0 μM), the lifetimes of Sender decrease from 5 to 4 h when increasing [S_T] from 5.0 to 40.0 μM (ratio of S_T to M_{RN2} from 0.5 to 4.0), because more reactive M_{R2} is produced and Receiver consumes more fuels. Additionally, the lag time shortens from 45 min to 15 min when increasing [S_T] to 40.0 μM. This is due to the fact that a higher [S_T] will accelerate the strand displacement reaction rate and thus gives a faster formation of M_{R2}. We note that the consistency within the parameter sweeps points to a high reproducibility and robustness of the system despite its complex multicomponent nature.

To broaden the accessible systems behavior, we next introduce RNase H, an endoribonuclease that specifically hydrolyzes RNA phosphodiester bonds in DNA-RNA hybrids to degrade RNA strands. The addition of this RNase sink now evolves the system towards a combination of two kinds of ERNs: (1) cyclic ligation/digestion ERNs running on NAD$^+$ (to steer Sender and Receiver), and (2) a non-cyclic ERN working as an RNA production/degradation scheme running on NTPs.

We hypothesized that this would allow more elaborate temporal control in the autonomous systems, as for instance the RNA-induced intermediate M_{RN1} (unreactive in Receiver) could be forced to be regenerated to the reactive M_{R1} to push the previously stopped Receiver back to an active state (Figure 3a). We call this process "Repression-Recovery". Experimentally, we added a large amount of NAD$^+$ (36.0 μM) to maintain Sender operational for long times during the experiments and to allow a focus on the repressed Receiver. [RNase H] was varied from very low (0.011 U μL^{-1}) to moderate (0.039 U μL^{-1}) and high concen-
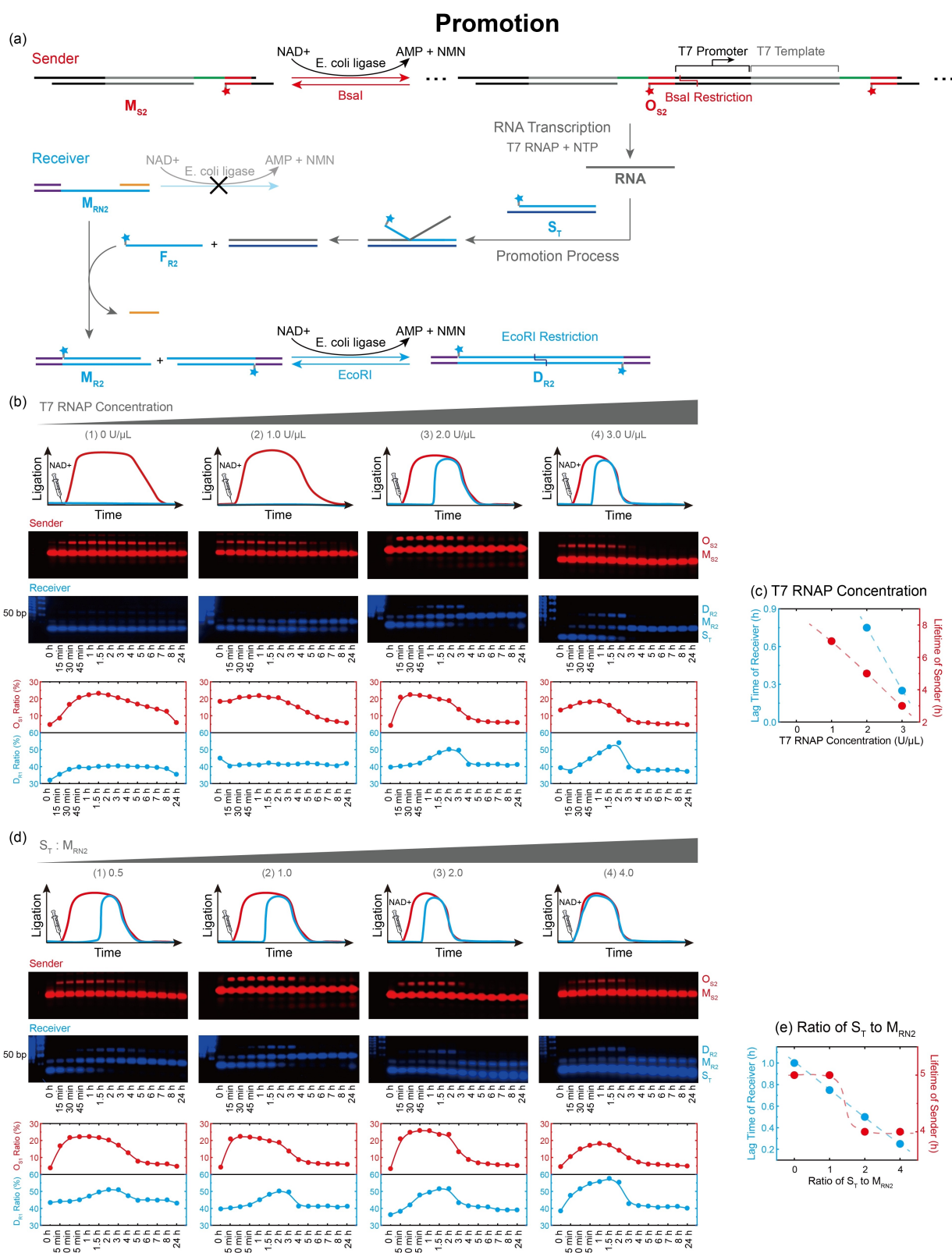
Promotion

Figure 2. Promotion. a) Schematic illustration of the promotion process between two ERNs. b) Time-dependent transient polymerization curves and time-dependent evolution of O_{S2} ratio ($[O_{S2}]/([O_{S2}]+[M_{S2}])$) and D_{R2} ratio ($[D_{R2}]/([D_{R2}]+[M_{R2}])$) as quantified by intensity analysis of the gel bands. c) Lifetime analysis of the promotion process with [T7 RNAP]. Other conditions: 10.0 µM M_{S2}, 10.0 µM M_{RN2}, 10.0 µM S_T, 10.0 U µL^{-1} ligase, 0.5 U µL^{-1} EcoRI, 1.5 U µL^{-1} BsaI, 2.0 mM NTP, and 9.0 µM NAD$^+$. d) Time-dependent transient polymerization curve and time-dependent evolution of O_{S2} ratio ($[O_{S2}]/([O_{S2}]+[M_{S2}])$) and D_{R2} ratio ($[D_{R2}]/([D_{R2}]+[M_{R2}])$) as quantified by intensity analysis of the gel bands. e) Lifetime analysis of the promotion process with different ratios of S_T to M_{RN2}. Other conditions: 10.0 µM M_{S2}, 10.0 µM M_{RN2}, 10.0 U µL^{-1} ligase, 0.5 U µL^{-1} EcoRI, 1.5 U µL^{-1} BsaI, 2.0 U µL^{-1} T7 RNAP, 2.0 mM NTP and 9.0 µM NAD$^+$.
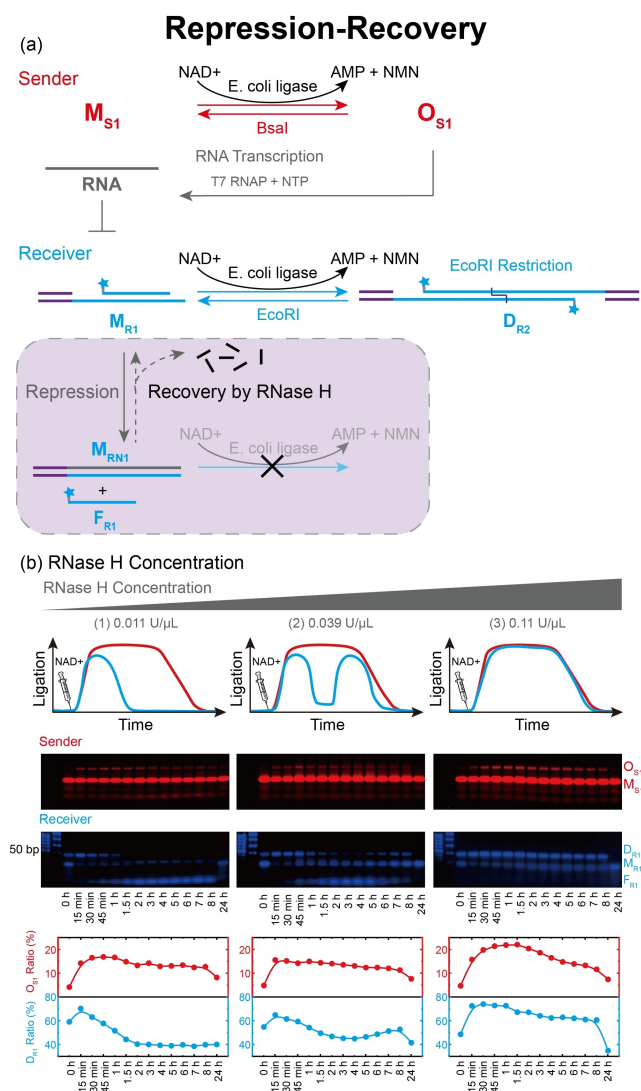
Figure 3. Repression-recovery. a) Schematic illustration of the repression-recovery process between two ERNs. b) Time-dependent transient polymerization curves of the repression-recovery process with [RNase H], and time-dependent evolution of O_{S1} ratio ($[O_{S1}]/([O_{S1}]+[M_{S1}])$) and D_{R1} ratio ($[D_{R1}]/([D_{R1}]+[M_{R1}]+[F_{R1}])$) as quantified by intensity analysis of the gel bands. Other conditions: 5.0 μM M_{S1}, 10.0 μM M_{R1}, 16.0 U μL^{-1} ligase, 0.67 U μL^{-1} EcoRI, 0.89 U μL^{-1} BsaI, 2.0 U μL^{-1} T7 RNAP, 2.0 mM NTP, and 36.0 μM NAD$^+$.

trations (0.11 U μL^{-1}; Figure 3b). Indeed, [RNase H] shows a profound influence. Three regimes can be distinguished. At very low [RNase H] of 0.011 U μL^{-1}, the behavior is qualitatively similar to systems without RNase H. The repression works effectively and the intermediately formed D_{R2} is effectively suppressed by the upstream RNA production (after 2 h). The fluorescent F_{R1} band (indicative of efficient RNA-mediated strand displacement) appears thereafter and exists for a long time (Figure 3b1). RNase H cannot provide a fast-enough digestion of the RNA in M_{RN1} to allow for reactivation of Receiver to the D_{R2} reporter. After 24 h, different from the repression process, the F_{R1} band disappears and M_{R1} reappears. This confirms that

RNase H digests the RNA bound to M_{RN1}, yet in a too slow manner to be relevant for the transient system.

Interestingly, in presence of moderate [RNase H] of 0.039 U μL^{-1}, a repression-recovery process appears (Figure 3b2). From 15 min to 5 h, the first round of a typical repression process occurs, with the D_{R1} band appearing at 15 min and disappearing at 2 h. The F_{R1} band appears at 45 min. However, after 5 h, the F_{R1} band gradually weakens and the D_{R1} band reappears, indicating substantial RNA degradation by RNase H and reengagement of the reformed M_{R1} into Receiver by strand displacement, resulting in a restart of Receiver. At 24 h, no F_{R1} remains, and only M_{R1} is left according to AGE, and the system returns to the initial state. The appearance of the two states can be explained by the fact that the RNA is generated quickly to take effect in Receiver, but then degraded on a system-relevant time scale.

The third situation can be induced upon addition of large quantities of RNase H of 0.11 U μL^{-1} (Figure 3b3). At this point, the hydrolysis rate of RNA by RNase H is so fast that the RNA-induced reconfiguration of reactive M_{R1} into M_{RN1} does not occur. There is hardly any band for F_{R1} visible, which is the strongest proof of a speedy recovery of M_{R1} from M_{RN1}. Note that RNase H is selective to RNA degradation on DNA. Consequently, Receiver runs similarly as Sender until the fuel (NAD$^+$) has run out.

At last, we introduce RNase H into the promotion process that works based on the signal transducer S_T to recode the RNA information for more elaborate control over the signal transducing events. Figure 4a displays that the addition of the RNase H can recover the intermediate S_I to S_T. Indeed, upon increasing [RNase H] from 0.011 U μL^{-1}, 0.028 U μL^{-1} to 0.05 U μL^{-1}, the lag times in Receiver increase from 30 min to infinity, as more S_T remains present in the solution. Since more [RNase H] suppresses efficient downstream activity of the produced RNA strand into Receiver, Sender shows a longer lifetime from 5 h to 6 h and 7 h, because less M_{R2} is generated and more NAD$^+$ fuel is available to Sender (Figure 4b).

Conclusion

In summary, we introduced conceptual and versatile strategies for the cross-regulation of two out-of-equilibrium ERNs yielding four different types of behavior (repression, promotion, repression-recovery, and promotion-stop) by on-demand integration of RNA transcription and degradation machinery. The communication occurs by conditional information exchange of RNA and RNA-mediated strand displacement reactions. The fuel-driven formation of the T7 promoter sequence in Sender is a key factor to initiate the cross-talk, as otherwise two independent ERN-based DySSs occur. The T7 RNAP concentration governs the RNA transcription rate and thereby the strength of communication, which effectively controls the lifecycles of both concatenated Sender and Receiver. A secondary cross-regulation occurs, because the NAD$^+$ fuel, originally shared equally between Sender and Receiver, becomes unequally
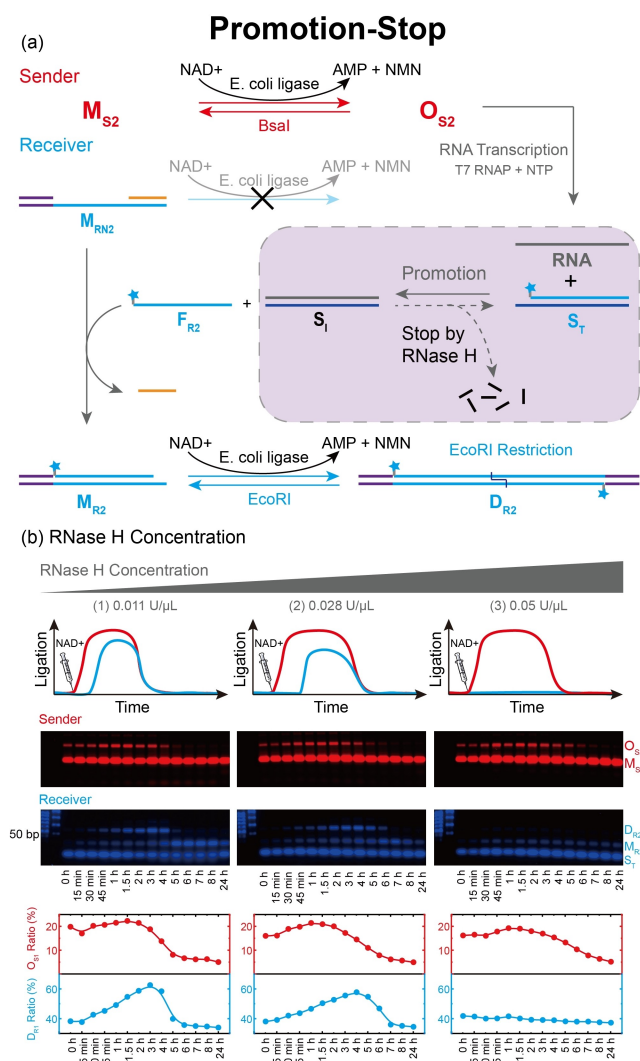
Figure 4. Promotion-stop. a) Schematic illustration of the promotion-stop process between two ERNs. b) Time-dependent transient polymerization curves of the promotion-stop process with [RNase H], and time-dependent evolution of O_{S2} ratio ($[O_{S2}]/([O_{S2}]+[M_{S2}])$) and D_{R2} ratio ($[D_{R2}]/([D_{R2}]+[M_{R2}])$) as quantified by intensity analysis of the gel bands. Other conditions: 10.0 μM M_{S2}, 10.0 μM M_{RN2}, 10.0 μM S_T, 10.0 U μL^{-1} ligase, 0.5 U μL^{-1} EcoRI, 1.5 U μL^{-1} BsaI, 2.0 U μL^{-1} T7 RNAP, 2.0 mM NTP, and 18.0 μM NAD$^+$.

In a wider perspective of systems chemistry, this work adds important regulatory control tools and another layer of complexity compared to typically operated individual cyclic reaction networks[5,11,15] which are important for the design of autonomous systems and more intelligent materials. Even though biological machinery and enzymes are robust tools for the implementation of such a communication and cross-regulation behavior, we believe that the guidelines provided here are also relevant to improve fully man-made regulatory networks in supramolecular chemistry, or even classic polymer chemistry. Besides, when incorporating with biological systems, this concatenated-network design can be a powerful tool as the regulator of the cellular bioactivities.

Acknowledgements

Conflict of Interest

The authors declare no conflict of interest.

Data Availability Statement

The data that support the findings of this study are available from the corresponding author upon reasonable request.

[1] E. Mattia, S. Otto, *Nat. Nanotechnol.* **2015**, *10*, 111–119.
[2] A. Walther, *Adv. Mater.* **2020**, *32*, 1905111.
[3] C. M. E. Kriebisch, A. M. Bergmann, J. Boekhoven, *J. Am. Chem. Soc.* **2021**, *143*, 7719–7725.
[4] G. Ragazzon, L. J. Prins, *Nat. Nanotechnol.* **2018**, *13*, 882–889.
[5] K. Das, L. Gabrielli, L. J. Prins, *Angew. Chem. Int. Ed.* **2021**, *60*, 20120–20143; *Angew. Chem.* **2021**, *133*, 20280–20303.
[6] A. Mishra, S. Dhiman, S. J. George, *Angew. Chem. Int. Ed.* **2021**, *60*, 2740–2756; *Angew. Chem.* **2021**, *133*, 2772–2788.
[7] Q. Wang, Z. Qi, M. Chen, D. H. Qu, *Aggregate* **2021**, *2*, e110.
[8] M. Weissenfels, J. Gemen, R. Klajn, *Chem* **2021**, *7*, 23–37.
[9] G. Ashkenasy, T. M. Hermans, S. Otto, A. F. Taylor, *Chem. Soc. Rev.* **2017**, *46*, 2543–2554.
[10] E. Del Grosso, L. J. Prins, F. Ricci, *Angew. Chem. Int. Ed.* **2020**, *59*, 13238–13245; *Angew. Chem.* **2020**, *132*, 13340–13347.
[11] J. Deng, A. Walther, *Adv. Mater.* **2020**, *32*, 2002629.
[12] N. Singh, G. J. M. Formon, S. De Piccoli, T. M. Hermans, *Adv. Mater.* **2020**, *32*, 1906834.

shared. This influences the lifetimes and the fractional degrees of ligation in Sender and Receiver. Adding a sink for the RNA messenger via RNase H allows to reach additional behavioral modes. In future, it will be important to develop full kinetic models allowing for a predictive behavior,[29] but at this point too many of the kinetic parameters, in particular for the NAD$^+$-driven ERNs, are still unknown and require substantial efforts to be obtained. These efforts are underway and will be published in a forthcoming article. A full model will likely be beneficial to further understand the robustness of oscillations and their potential implementation in a continuously stirred tank reactor under open conditions.

[13] J. H. van Esch, R. Klajn, S. Otto, *Chem. Soc. Rev.* **2017**, *46*, 5474–5475.

[14] I. Hwang, R. D. Mukhopadhyay, P. Dhasaiyan, S. Choi, S. Y. Kim, Y. H. Ko, K. Baek, K. Kim, *Nat. Chem.* **2020**, *12*, 808–813.

[15] B. Rieß, R. K. Grötsch, J. Boekhoven, *Chem* **2020**, *6*, 552–578.

[16] E. Del Grosso, I. Ponzo, G. Ragazzon, L. J. Prins, F. Ricci, *Angew. Chem. Int. Ed.* **2020**, *59*, 21058–21063; *Angew. Chem.* **2020**, *132*, 21244–21249.

[17] S. Dhiman, A. Jain, S. J. George, *Angew. Chem. Int. Ed.* **2017**, *56*, 1329–1333; *Angew. Chem.* **2017**, *129*, 1349–1353.

[18] M. P. van der Helm, C.-L. Wang, B. Fan, M. Macchione, E. Mendes, R. Eelkema, *Angew. Chem. Int. Ed.* **2020**, *59*, 20604–20611; *Angew. Chem.* **2020**, *132*, 20785–20792.

[19] S. P. Afrose, C. Mahato, P. Sharma, L. Roy, D. Das, *J. Am. Chem. Soc.* **2022**, *144*, 673–678.

[20] S. Choi, R. D. Mukhopadhyay, Y. Kim, I.-C. Hwang, W. Hwang, S. K. Ghosh, K. Baek, K. Kim, *Angew. Chem. Int. Ed.* **2019**, *58*, 16850–16853; *Angew. Chem.* **2019**, *131*, 17006–17009.

[21] H. Che, S. Cao, J. C. van Hest, *J. Am. Chem. Soc.* **2018**, *140*, 5356–5359.

[22] L. Heinen, A. Walther, *Soft Matter* **2015**, *11*, 7857–7866.

[23] Z. Zhou, Y. Ouyang, J. Wang, I. Willner, *J. Am. Chem. Soc.* **2021**, *143*, 5071–5079.

[24] A. Baccouche, K. Montagne, A. Padirac, T. Fujii, Y. Rondelez, *Methods* **2014**, *67*, 234–249.

[25] T. Fujii, Y. Rondelez, *ACS Nano* **2013**, *7*, 27–34.

[26] A. Zadorin, Y. Rondelez, G. Gines, V. Dilhas, G. Urtel, A. Zambrano, J.-C. Galas, A. Estevez-Torres, *Nat. Chem.* **2017**, *9*, 990–996.

[27] G. Gines, A. S. Zadorin, J.-C. Galas, T. Fujii, A. Estevez-Torres, Y. Rondelez, *Nat. Nanotechnol.* **2017**, *12*, 351–359.

[28] S. W. Schaffter, R. Schulman, *Nat. Chem.* **2019**, *11*, 829–838.

[29] L. N. Green, H. K. K. Subramanian, V. Mardanlou, J. Kim, R. F. Hariadi, E. Franco, *Nat. Chem.* **2019**, *11*, 510–520.

[30] L. Heinen, A. Walther, *Sci. Adv.* **2019**, *5*, eaaw0590.

[31] J. Deng, D. Bezold, H. J. Jessen, A. Walther, *Angew. Chem. Int. Ed.* **2020**, *59*, 12084–12092; *Angew. Chem.* **2020**, *132*, 12182–12190.

[32] J. Deng, A. Walther, *Nat. Commun.* **2020**, *11*, 3658.

[33] J. Deng, A. Walther, *Chem* **2020**, *6*, 3329–3343.

[34] J. Deng, A. Walther, *J. Am. Chem. Soc.* **2020**, *142*, 685–689.

[35] M. Sun, J. Deng, A. Walther, *Angew. Chem. Int. Ed.* **2020**, *59*, 18161–18165; *Angew. Chem.* **2020**, *132*, 18318–18322.

[36] J. Deng, A. Walther, *Nat. Commun.* **2021**, *12*, 5132.

[37] J. Heckel, F. Batti, R. T. Mathers, A. Walther, *Soft Matter* **2021**, *17*, 5401–5409.

[38] S. Groeer, K. Schumann, S. Loescher, A. Walther, *Sci. Adv.* **2021**, *7*, eabj5827.

[39] J. Deng, A. Walther, *J. Am. Chem. Soc.* **2020**, *142*, 21102–21109.